Open Archive TOULOUSE Archive Ouverte (OATAO)

OATAO is an open access repository that collects the work of Toulouse researchers and makes it freely available over the web where possible.

Any correspondence concerning this service should be sent to the repository administrator: staff-oatao@listes-diff.inp-toulouse.fr

Full Length Article

Tar conversion over olivine and sand in a fluidized bed reactor using toluene as model compound

Mathieu Morin*, Xavier Nitsch, Sébastien Pécate, Mehrdji Hémati

Laboratoire de Génie Chimique, Université de Toulouse, CNRS, INPT, UPS, 4 allée Emile Monso, 31432 Toulouse, France

ABSTRACT

Keywords:
Tar removal
Steam reforming
Fluidized bed
Biomass gasification
Catalyst

The aim of this work is to study the tars conversion in conditions representative of biomass gasification in a fluidized bed reactor. Experiments are conducted at 850 °C and atmospheric pressure in a fluidized bed reactor with toluene as tar model. Influences of the nature of the media (sand and olivine) and of the reactive atmosphere (steam and hydrogen partial pressures) on toluene conversion are particularly studied. The steam and hydrogen partial pressures were varied in the range of 0.05 to 0.4 bars and 0 to 0.2 bars, respectively. Results showed a strong influence of these parameters on toluene conversion. Olivine was found to have a catalytic activity towards steam reforming reactions which depends on the ratio P_{H_2}/P_{H_2O} in the reactor. Both thermo-dynamic equilibrium and surface analyses (EDX and XRD) of olivine particles suggested that this ratio controls the oxidation/reduction of iron at the olivine surface. Besides, iron is more active towards tars removal when its oxidation state is low. At 850 °C and $P_{H_2}/P_{H_2O} > 1.5$, the iron is reduced to form native iron (Fe^0) on the olivine surface which favors the steam reforming of toluene.

1. Introduction

Biomass gasification is considered as a promising alternative route to replace fossil energy for the production of syngas. It is a thermo-chemical conversion occurring at high temperatures with many si-multaneous reactions. Fig. 1 presents a simplified diagram which de-scribes the biomass transformations in successive steps according to the temperature and the reactive atmosphere.

(i) For temperatures above 350 °C, biomass undergoes a fast thermal conversion. This pyrolysis step converts the biomass into volatile products, either condensable (steam and primary tars) or non-condensable (H_2, CO, CO_2, CH_4 and C_2H_x) and a solid residue called char [1].

(ii) For temperatures greater than 700 °C, the gasification step con-verts the char into synthesis gas by reaction with steam and carbon dioxide.

(iii) Milne and Evans [2] suggested that tars from biomass pyrolysis can be classified as primary, secondary and tertiary tars according to the reactor temperature. Primary tars are a mixture of oxygenated compounds coming from cellulose, hemicellulose and lignin con-versions. The decomposition of cellulose and hemicellulose mainly leads to the formation of levoglucosan, hydroxyaldehydes and furfurals while methoxyphenols are mostly produced from the conversion of lignin. Above 500 °C, primary tars are converted into secondary tars which are characterized by phenolic and olefin compounds. Finally, for temperatures above 750 °C, the primary tars are completely destroyed and the tertiary tars appear. They include methyl derivatives of aromatics and Polycyclic Aromatic Hydrocarbon (PAH) series without substituents.

The reactive system of biomass conversion (i.e. pyrolysis and gasi-fication) is an endothermic process. A contribution of energy is neces-sary in order to maintain the temperature and the different reactions in the reactor. One of the most promising technologies for biomass gasi-fication at large-scale is dual fluidized bed (Fast Internally Circulating Fluidized Bed, FICFB). It consists of two interconnected reactors: a dense fluidized bed endothermic gasifier (operating around 850 °C) which produces the syngas from biomass gasification, and an entrained bed exothermic reactor that burns a part of the residual char to provide heat to the gasifier. A bed material (sand, olivine or catalyst particles) circulates between the two reactors to transfer the heat.

During biomass gasification, the high temperature in the gasifier leads to the presence of refractory tars (tertiary tars) which con-taminates the finally produced synthesis gas [3]. Indeed, they may lead to condensation, polymerization and clogging in the exit pipes. For instance, Table 1 gives the maximum tars concentration acceptable for different syngas applications. Besides, the works of de Sousa [4]
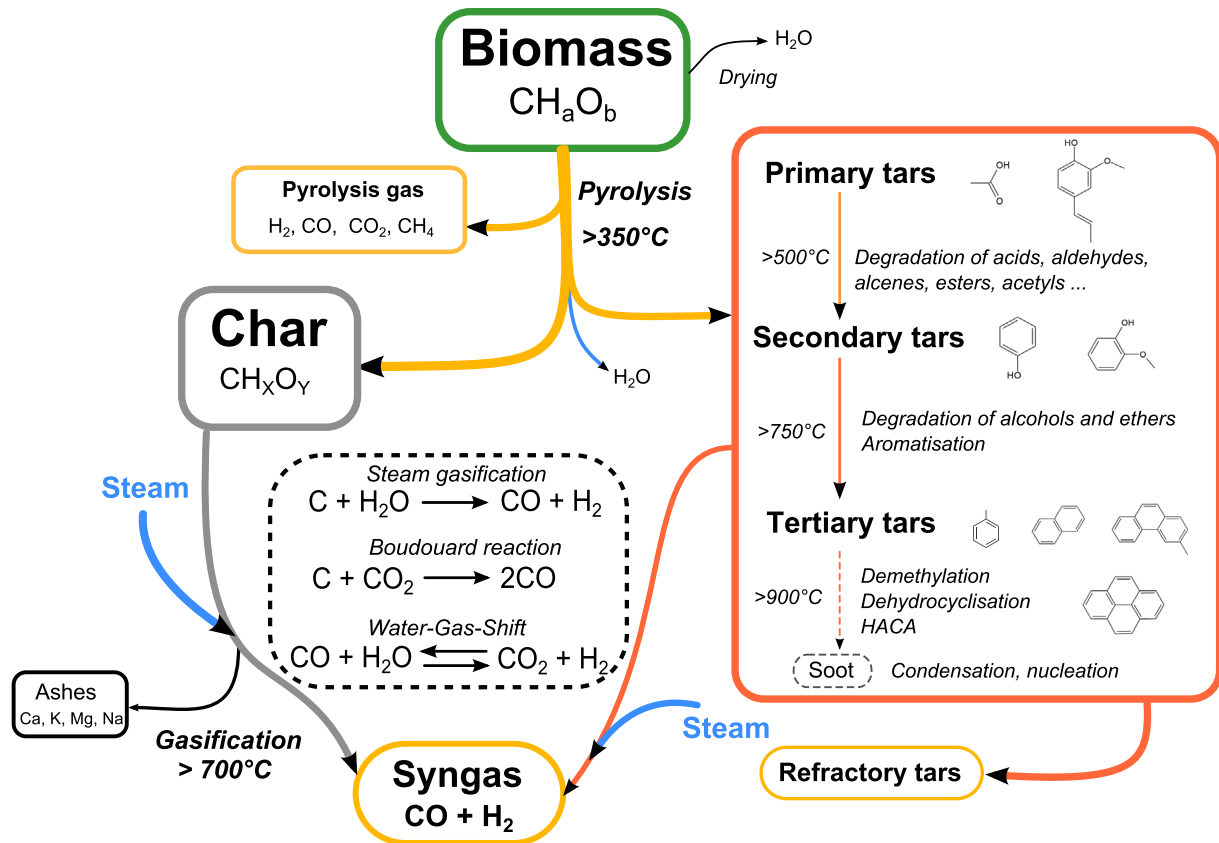
Fig. 1. Diagram of steam gasification of biomass and tars formation.

showed that, for gasification experiments in a fluidized bed reactor, the main tertiary tars are benzene, toluene and naphthalene.

The removal of tars is a primordial technological barrier hindering the development of biomass gasification. Several approaches for tars removal can be found in the literature and are classified into two types: treatment inside the gasifier itself (primary methods) or gas cleaning outside the gasifier (secondary methods) [5]. The secondary methods include tars removal through chemical treatments either thermally or catalytically, or physical treatments such as tars condensation, gas/liquid separations or filtration [2]. Tars removal by secondary methods have been widely investigated and are well established in the literature [2,5]. The primary treatments may have the advantages in eliminating the use of downstream cleanup processes and depend on the operating conditions, the type of bed particles and the reactor design.

The use of catalytic solids in the gasifier has shown to be one of the best approaches to reduce tars content in the syngas [6]. Various catalysts were investigated in biomass gasification for tars conversion and have been discussed in several reviews [5,7–9]. Among them, calcined dolomite and olivine as well as Ni-based catalysts were found to have a strong catalytic activity.

A general agreement is drawn in the literature on the significant effect of dolomite as tars removal catalyst [10–13]. This natural solid is relatively inexpensive and disposal. Its calcination at high temperatures leads to the decomposition of the carbonate mineral to form MgO-CaO which is the main active catalytic component. However, this solid is not

appropriate for use in fluidized bed reactors due to its low attrition resistance.

Olivine is another natural inexpensive and disposable mineral with a global formula $(Mg_xFe_{1-x})_2SiO_4$. Many studies were carried out to determine and understand the catalytic effect of olivine [10,14–23]. For instance, some authors [12,18–23] compared results obtained from biomass gasification in a fluidized bed reactor with either olivine or inert sand particles. They concluded that the presence of olivine in the reactor leads to a lower tars content, a higher syngas yield, an increase in the H_2 and CO_2 content and a decrease in the amount of CO and CH_4. They attributed this effect to the catalytic activity of olivine towards the tars removal and the Water-Gas-Shift reaction (Reaction (III)). In the literature [15,24], the catalytic performance of olivine is related to the presence of segregated iron at the particle surface which may have different oxidation states (i.e. iron(III), iron(II) and native iron). Devi et al. [15] mentioned that the calcination of olivine prior to experiments is essential and the presence of segregated iron is optimal for calcination at 900 °C and 10 h. For olivine calcination between 400 and 1100 °C, a part of the iron is ejected from the olivine structure according to the following reaction [24,25]:

$$(Mg_xFe_{1-x})_2SiO_4 + \frac{1-x}{2}O_2 \rightarrow xMg_2SiO_4 + (1-x)Fe_2O_3 + (1-x)SiO_2$$

(I)
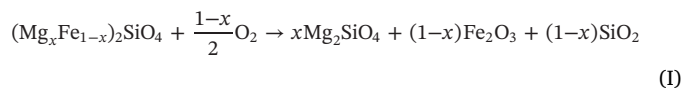
Under reducing atmosphere, the reduction of Fe_2O_3 occurs in two steps [24,25]:

- the reduction of Fe_2O_3 into Fe_3O_4 for temperatures between 350 and 500 °C,
- the reduction of Fe_3O_4 into FeO and $\alpha-Fe$ between 500 and 900 °C.

Several researchers [11,17,26] concluded that iron is more active towards tars removal when its oxidation state is low. For instance,

~

metal iron (α−Fe) was found to be an active phase for C−C and C−H bonds breaking in hydrocarbons [25,27,28]. Hence, the reactive gas atmosphere (i.e. oxidizing or reducing) is a key parameter for the catalytic activity of olivine. During phenol-based tars conversion over olivine and sand at 850 °C, Nitsch et al. [14] concluded that high steam partial pressures promote the oxidation of olivine and hinders its catalytic activity while low pressures give reduced active sites and a high activity in steam reforming of tars. Consequently, the authors described a mechanism of the catalytic decomposition of tars over olivine similar to the one proposed by Uddin et al. [29]. The reaction scheme suggested that reduced irons on the olivine surface yield to tars polymerization by cracking or cokefaction reactions followed by the steam gasification/reforming of the carbonaceous solid deposit. Overall, bibliographic works concluded that olivine has a higher mechanical resistance but a slightly lower activity in tars removal compared to dolomite [9,12,18]. For instance, in the case of biomass gasification with air in a fluidized bed reactor, Corella et al. [10] reported that dolomite is 1.4 times more effective for in-bed tars removal than olivine but it generates 4–6 times more fine particulates in the gasification gas. In the case of gasification in FICFB process, the solid medium resistance to attrition phenomena is a key parameter. Therefore, olivine seems to be the best compromise compared to dolomite.

Ni-based catalysts were widely investigated in the literature for tars conversion from biomass gasification [18,30–32]. This material showed a strong catalytic effect in steam reforming of both hydrocarbons and methane. Besides, at high temperatures, nickel may favor the formation of hydrogen and carbon monoxide in the exiting gas. The two major problems with Ni-based catalysts are the fast deactivation due to carbon deposition on the solid surface and its lower resistance to attrition in fluidized bed reactors compared to olivine.

During toluene conversion, many parallel and consecutive reactions can take place [30,33,34]. Toluene may react with steam to produce H_2 and CO according to the global steam reforming reaction:

$$C_7H_8 + 7H_2O \rightarrow 7CO + 11H_2 \tag{II}$$

The Water-Gas-Shift reaction (WGS) occurs simultaneously:

$$CO + H_2O \leftrightarrow CO_2 + H_2 \tag{III}$$

In reality, some works in the literature [14,29] suggested that Reaction (II) may be divided into two different reactions in series: the carbonaceous solid deposition on the solid surface by tars polymerization or cokefaction followed by the steam gasification/reforming of the carbonaceous solid.

Other reactions must be considered during toluene conversion in the presence of steam and hydrogen. Toluene can react with steam to produce benzene, CO and H_2 from the reaction of steam dealkylation (Reaction (IV)) or with hydrogen to form benzene and methane according to the hydrodealkylation reaction (Reaction (V)) [35]:

$$C_7H_8 + H_2O \rightarrow C_6H_6 + CO + 2H_2 \tag{IV}$$

$$C_7H_8 + H_2 \rightarrow C_6H_6 + CH_4 \tag{V}$$

The purpose of the present paper is to study the cracking and reforming of tar in conditions representative of biomass gasification in a fluidized bed reactor. Toluene is used as tertiary tar model. The effect of the solid medium (sand and olivine) and the reactive atmosphere (steam and hydrogen partial pressures) in the fluidized bed reactor on toluene conversion is particularly studied. Experiments are carried out at 850 °C and at atmospheric pressure. Effects of steam partial pressure ranging from 0.05 to 0.4 bars and hydrogen partial pressure between 0 and 0.2 bars are investigated. The catalytic effect of olivine is highlighted by EDX and XRD analyzes combined to the thermodynamic equilibrium of iron. Finally, a schematic diagram of the catalytic conversion of tars over olivine is proposed.

Table 2
Physicochemical properties of the solid media.

Particles type	d_{32}	True density ρ_t	Apparent density ρ_p	Porosity ε_p	U_{mf} (850 °C)
	(µm)	(kg.m^{-3})	(kg.m^{-3})	(%)	(m.s^{-1})
Sand	246	2650 ± 2	2400 ± 20	9	2.9
Olivine	264	3265 ± 2	2965 ± 20	9	3.7

2. Experimental section

2.1. Solid media

The physicochemical properties of the solid particles used as fluidized media are given in Table 2. The apparent and true densities were determined from mercury porosimetry and helium pycnometry, respectively. ε_p corresponds to the porosity of a single particle (sand or olivine) and was calculated from values of the apparent and the true density.

Olivine was purchased from the Austrian company Magnolithe Gmbh. After receipt, the particles were calcined at 900 °C for 4 h in a fluidized bed reactor before being sieved between 200 and 300 µm. Its composition were characterized after calcination by 19.4 wt% of Si, 31.4 wt% of Mg, 41.9 wt% of O and 6.8% of Fe [14]. In the following, this olivine will be referred to "calcined olivine". The minimum fluidization velocity (U_{mf}) of olivine was measured experimentally with nitrogen and is equal to 3.7 cm/s at 850 °C.

Sand was calcined following the same procedure and sieved to obtain particles size between 200 and 300 µm.

2.2. Experimental setup

The experimental setup is shown in Fig. 2. The fluidized bed reactor consists of a tube of internal diameter of 5.26 cm and a height of 94 cm heated by an electric furnace delivering 2.6 kW of electric power. About 580 g of solids particles (sand or olivine) are used as fluidized solids.

The reactor is supplied with N_2, H_2, H_2O and toluene. The nitrogen and hydrogen flow rates are carefully regulated by two mass flowmeters Aera FC-7700-CD. H_2O is fed by a pump Gilson 305 100SC. The feeding gases are preheated between 200 and 300 °C in a stainless steel tube forming a coil around the reactor. The coil is supplied with liquid water which is continuously vaporized. Then, preheated gases enter in a wind box beneath the reactor in which the toluene is continuously injected by a pump Gilson 305 25SC. The wind box is partially filled with porous silicon carbide (SiC). This structure is used as a mixing zone and favors the toluene vaporization. The gas distribution in the bed is done by a perforated plate of 19 orifices equipped at its base by a stainless steel sieve with 30 µm of mesh.

The temperature inside the fluidized bed is controlled by two thermocouples located at 5 and 25 cm above the distributor. The former is used to regulate the temperature of the reactor using a PID controller. A differential pressure transmitter is connected at 5 and 500 mm above the distributor in order to follow the pressure drop of the bed. At the reactor outlet, the elutriated particles and the condensable gases are collected by a cyclone and a condenser, respectively.

2.3. Sampling method and gas analysis

The sampling of gases is carried out by a stainless steel mobile probe located at the fluidized bed surface. A thermocouple is placed inside the mobile probe to measure the precise temperature at the entrance of the probe. The gas sample is sucked by a vacuum pump connected to a flowmeter (constant volume flow rate of 100 mL.min^{-1} at STP). At the mobile probe outlet, the pumped gas passes through a cyclone and a filter to separate gas from particles and through a wash-bottle cooled at
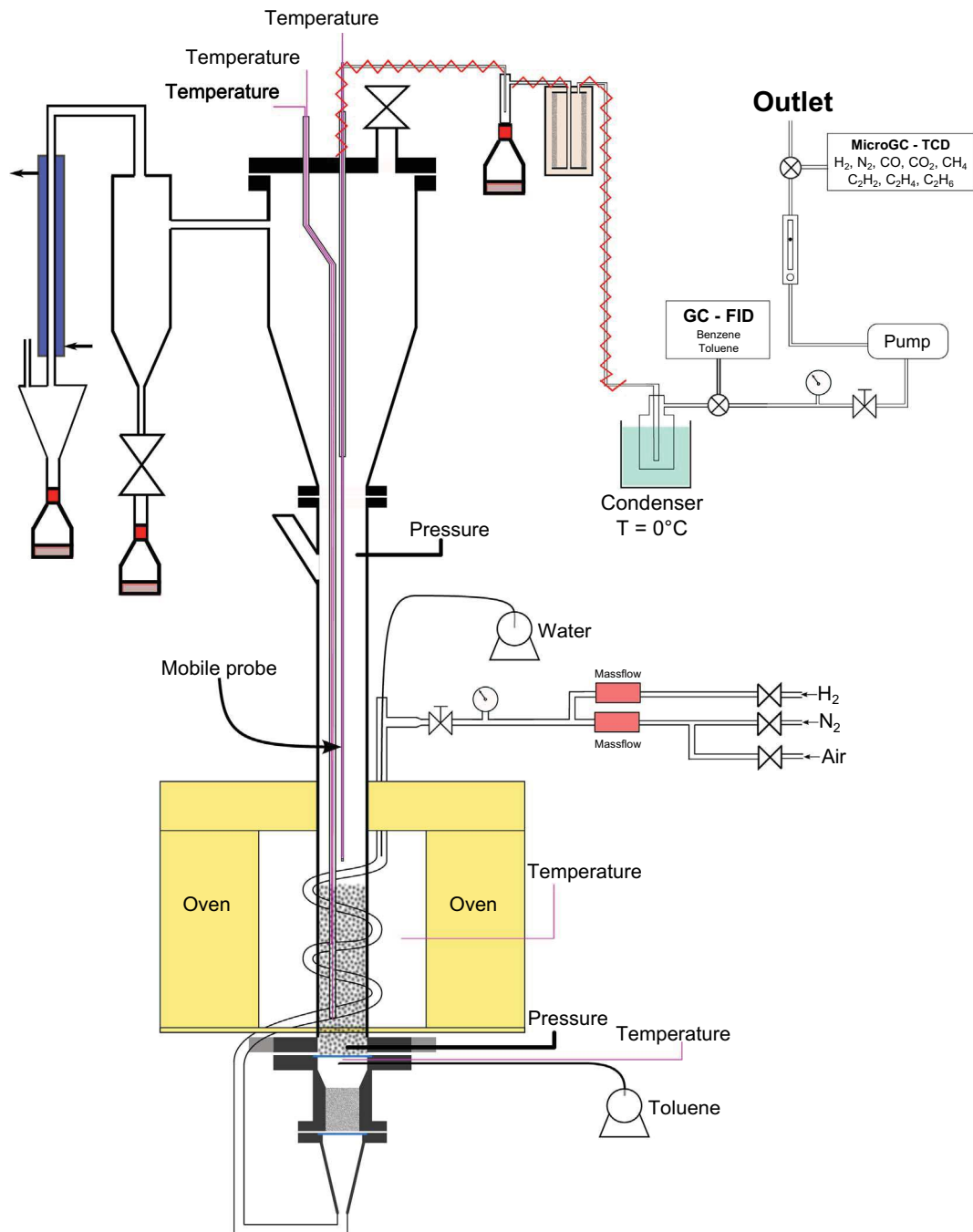
Fig. 2. Experimental setup used for toluene conversion.

0 °C to remove any traces of water. At this temperature, the theoretical condensation of toluene occurs when its partial pressure exceeds 0.0093 bars. To prevent any condensation of steam, all of the lines from the reactor to the entrance of the condensation system are heated to a temperature of 150 °C.

The sample is sent online to a Gas Chromatograph (GC) Thermoscience Trace GC Ultra equipped with a 30 m × 0.53 mm ID 0.5 μm capillary TR-5 column with 5% Phenyl Methylpolysiloxane heated at 60 °C for 6 min. A Flame Ionization Detector (FID) enables to quantify both benzene and toluene.

A micro Gas Chromatograph (micro GC) is used to online analyze the non-condensable gases. It is equipped with a Poraplot U 10 m × 0.25 mm ID column connected to a Thermal Conductivity Detector (TCD) calibrated for CO_2 quantification. A CP-Molsieve 5 A 10 m × 0.25 mm column connected to a TCD is calibrated for the

analyses and quantification of N_2, H_2, O_2, CH_4 and CO. The time-lapse between two quantifications is about 3 min.

2.4. Operating conditions and data treatments

The tests were conducted at atmospheric pressure and a temperature of 850 °C. The total molar flow rate at the entrance of the reactor was kept constant and equal to 0.35 $mol.min^{-1}$ so that the gas velocity was set to 7 times the minimum fluidization velocity of olivine at 850 °C. In this case, the bed porosity has been determined experimentally and is equal to 0.6. Based on literature data regarding the amount of tars during biomass gasification [2,4], the toluene partial pressure in the reactor was fixed to 0.005 bar which corresponds to 20.3 $g.Nm^{-3}$. The effect of solid media was studied using sand and olivine particles while the influence of steam and hydrogen partial pressures was

Table 3
Operating conditions of each experiment, 850 °C and F_{total} = 0.35 mol.min^{-1}, (experimental error on X_c corresponds to the uncertainty due to replicate experimental measurements).

Exp.	P$_{H2}$	P_{H_2O}	P$_{N2}$	P$_{C7H8}$	Medium	P_{H_2}/P_{H_2O}	X$_c$
–	(bar)	(bar)	(bar)	(bar)	–	(–)	(%)
S_1a	0	0.4	0.595	0.005	Sand	0	3.9
S_1b	0	0.2	0.795	0.005	Sand	0	3.7
S_1c	0	0.1	0.895	0.005	Sand	0	4.3 ± 0.5
S_1d	0	0.05	0.945	0.005	Sand	0	4
S_2a	0	0.1	0.895	0.005	Sand	0	4.3 ± 0.5
S_2b	0.05	0.1	0.845	0.005	Sand	0.5	17.8
S_2c	0.1	0.1	0.795	0.005	Sand	1	24.6
S_2d	0.2	0.1	0.695	0.005	Sand	2	33.9
O_1a	0	0.4	0.595	0.005	Olivine	0	32.7
O_1b	0	0.2	0.795	0.005	Olivine	0	30.9
O_1c	0	0.1	0.895	0.005	Olivine	0	33 ± 3.5
O_1d	0	0.05	0.945	0.005	Olivine	0	27.1
O_2a	0	0.1	0.895	0.005	Olivine	0	33 ± 3.5
O_2b	0.05	0.1	0.845	0.005	Olivine	0.5	36.4
O_2c	0.1	0.1	0.795	0.005	Olivine	1	42.6
O_2d	0.2	0.1	0.695	0.005	Olivine	2	90 ± 1
O_3a	0.2	0.4	0.395	0.005	Olivine	0.5	40.0
O_3b	0.2	0.2	0.595	0.005	Olivine	1	40.9
O_3c	0.2	0.1	0.695	0.005	Olivine	2	90 ± 1
O_3d	0.2	0.05	0.745	0.005	Olivine	4	99.5

investigated in the range of 0 to 0.4 bars and 0 to 0.2 bars, respectively.

The different operating conditions of each experiment are presented in Table 3.

For each experiment, the composition of both the non-condensable gases and the tars are analyzed as a function of time. The nitrogen is not involved during the toluene conversion and is only used as an inert gas for mass balances. Once a steady state is achieved (i.e. no variation in the molar fractions of each component), the molar fractions of each component are averaged and the total molar flow rate is calculated according to the following expression:

$$\dot{n}_t = \frac{\dot{n}_{N_2}}{x_{N_2}}$$
(1)

where $\dot{n}_t$ is the total molar flow rate (mol.min^{-1}), $\dot{n}_{N_2}$ represents the molar flow rate of nitrogen at the entrance of the reactor (mol.min^{-1}) and x_{N_2} is the averaged measured molar fraction of nitrogen at the reactor outlet.

The partial molar flow rate of each component is calculated as follows:

$$\dot{n}_i = x_i \cdot \dot{n}_t$$
(2)

where $\dot{n}_i$ and x_i are the partial molar flow rate and the averaged molar fraction of component i at the reactor outlet, respectively ($i = C_6H_6, CO, CO_2, CH_4$ and C_7H_8).

The normalized distribution of carbon-containing species at the reactor outlet is given by the following expression:

$$X_i = \frac{\dot{n}_i \cdot \gamma_i}{7 \cdot \dot{n}_{C_7H_8}^{in}}$$
(3)

where γ_i represents the number of carbon atoms in the component i and $\dot{n}_{C_7H_8}^{in}$ is the toluene molar flow rate at the entrance of the reactor (mol.min^{-1}).

It is important to note that $X_{toluene}$ given in Eq. (3) corresponds to the amount of toluene which was not converted during the experiment.

The toluene conversion, noted X_c, is defined as the ratio between the total carbon molar flow rate of produced species C_6H_6, CO, CO_2 and CH_4 and the carbon molar flow rate of introduced C_7H_8.

$$X_c = 1 - X_{toluene} = \frac{6 \cdot \dot{n}_{C_6H_6} + \dot{n}_{CO} + \dot{n}_{CO_2} + \dot{n}_{CH_4}}{7 \cdot \dot{n}_{C_7H_8}^{in}}$$
(4)

Finally, selectivities of carbon-containing products are defined according to the equation below:

$$S_j = \frac{\dot{n}_j \cdot \gamma_j}{7 \cdot (\dot{n}_{C_7H_8}^{in} - \dot{n}_{C_7H_8})}$$
(5)

where S_j is the selectivity of component j ($j = C_6H_6$, CO, CO_2 and CH_4).

Each experiment obtained a total molar carbon balance between 91 and 104%. These small deviations may originate from two different phenomena:

- the small variation in the piston pumps which supply liquid toluene and water to the reactor;
- the carbon formation on the solid surface by tars polymerization or cokefaction. However, some authors in the literature [14] reported that carbon deposition remains low in the presence of steam.

Therefore, carbon deposition on the solid surface was not considered in the carbon balance calculation.

Besides, some experiments (i.e. experiments S_1c and S_2a, O_1c and O_2a, and O_2d and O_3c, see Table 3) have been repeated with a time lapse of 2 months. The results showed a very good repeatability of the replicate experimental measurements. Besides, for these replicate experiments, an average value of X_i, X_c and S_j has been taken into account.

2.5. Characterization techniques

Samples of calcined olivine and olivine recovered after the experiment O_3d were analyzed in order to identify iron-rich zones and to determine the oxidation state of the free iron at the solid surface. These olivine particles have a spheroidal shape with a diameter between 200 and 300 μm. The samples were characterized through different techniques:

- Scanning Electron Microscopy (SEM) and Energy-dispersive X-ray spectroscopy (EDX) on a SEM FEG JSM 7100 FTTLS apparatus,
- X-ray diffraction (XRD) on a Bruker instrument using Cu Kα radiation with a wavelength of 1.5418 Å in order to observe the presence of crystalline phase. The diffractograms were recorded between 10 and 50°.

2.6. Thermodynamic equilibrium of iron

The thermodynamic equilibrium of iron was calculated with the software HSC Chemistry 5.11 in order to highlight the effect of H_2O and H_2 on the oxidation and reduction of iron. At the initial state, the presence of Fe, O and H elements is considered. The amount of H_2O is fixed while the one of H_2 continuously increased. Besides, H_2 and H_2O are taken in large excess compared to iron. Toluene is not considered in the reactive gases since its presence leads to the formation of CO and H_2.

The calculation is based on the minimization of the Gibbs free energy. For a closed system with N_c compounds, this energy is calculated as:

$$G = \sum_{i=1}^{N_c} n_i \cdot (\mu_i^0 + RT ln(a_i))$$
(6)

With G the Gibbs energy (J), n_i the amount of i in the system (mol), μ_i^0 is the standard chemical potential of i (J.mol^{-1}), R is the universal gas constant (J.mol^{-1}.K^{-1}) and a_i is the activity of i.
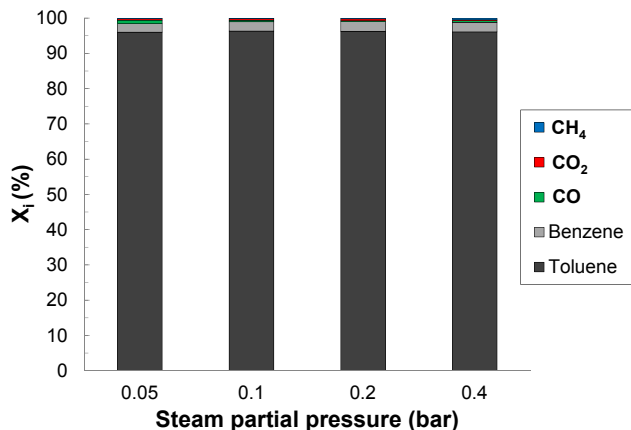
Fig. 3. Effect of steam partial pressure on the normalized distribution of carbon-containing species during toluene conversion with sand particles (experiments S_1).

3. Results and discussion

3.1. Experiments with sand particles

Toluene degradation in the fluidized bed reactor was investigated at 850 °C for different steam and hydrogen partial pressures with sand as fluidized particles.

Fig. 3 presents the effect of steam partial pressure between 0.05 and 0.4 bars on toluene conversion. It can be seen that 96% of the toluene introduced in the reactor is not converted. The toluene conversion X_c less than 4% gave rise to the formation of a very small amount of benzene and CO. This formation may originate from the reaction of steam dealkylation (Reaction (IV)). Besides, an increase in the steam partial pressure does not reveal any influences on toluene conversion.

The effect of hydrogen partial pressure was studied in the range of 0–0.2 bars for a constant steam partial pressure of 0.1 bars. The results are given in Fig. 4. It emphasizes that an increase in the hydrogen partial pressure leads to a higher toluene conversion. For instance, the toluene conversion is equal to 4, 18, 25 and 34% for a hydrogen partial pressure of 0, 0.05, 0.1 and 0.2 bars, respectively. Besides, this figure shows that the main carbonaceous produced compounds are benzene, CO, CO_2 and CH_4. Fig. 5 presents the produced molar flow rates of both benzene and CH_4 versus hydrogen partial pressure. The two molar flow rates were found to be very close to each other. This indicates that the presence of C_6H_6 and CH_4 are the results of the hydrodealkylation of toluene in the presence of hydrogen according to Reaction (V). The small interval observed in Fig. 5 may originate from Reaction (IV)
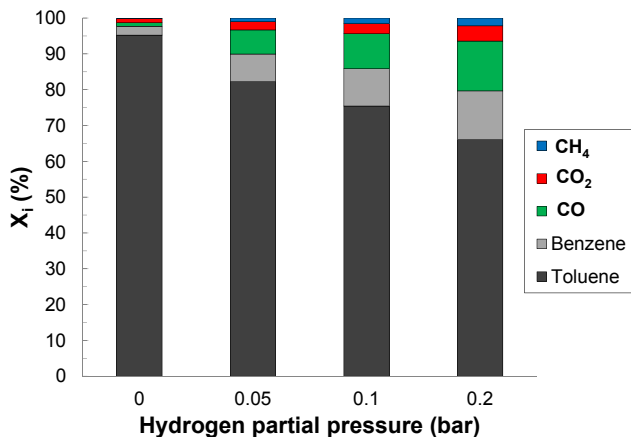

Fig. 4. Effect of hydrogen partial pressure on the normalized distribution of carbon-containing species during toluene conversion with sand particles (experiments S_2 with $P_{H_2O} = 0.1$ bars).
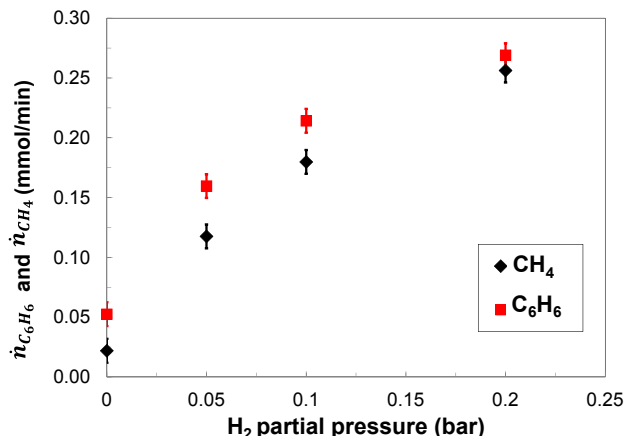

Fig. 5. Molar flow rates of benzene and methane versus hydrogen partial pressure (experiments S_2 with $P_{H_2O} = 0.1$ bars), the error bars correspond to the uncertainty due to replicate experimental results.

which is thermodynamically favored at low hydrogen partial pressures.

3.2. Experiments with olivine particles

Three sets of experiments were conducted with olivine as fluidized medium (i.e. experiments O_1, O_2 and O_3, see Table 3).

Fig. 6 (A) illustrates the influence of steam partial pressure on the normalized distribution of carbon-containing species during the
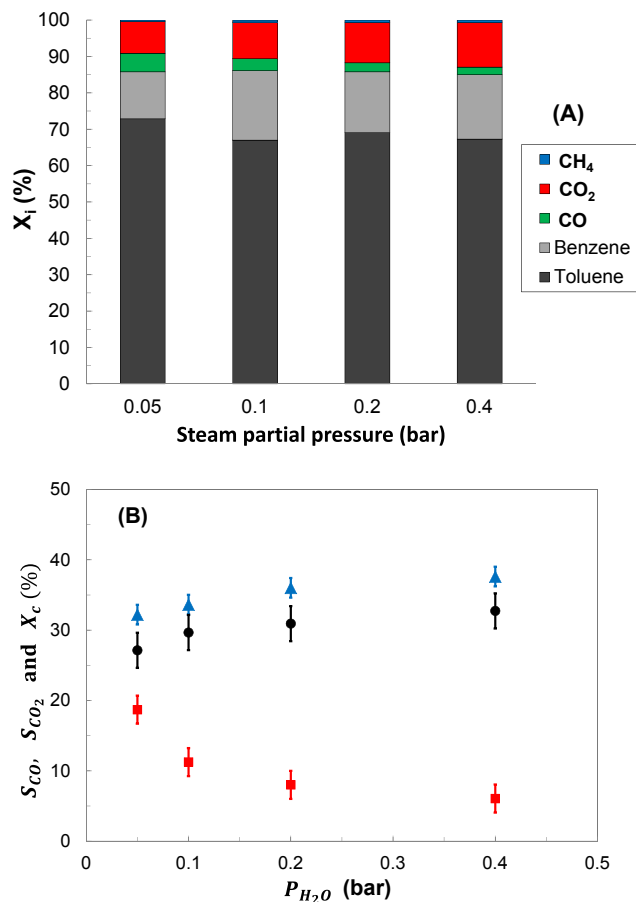

Fig. 6. Effect of steam partial pressure on toluene conversion, (A) Normalized distribution of carbon-containing products, (B) selectivities of CO and CO_2 and toluene conversion versus steam partial pressure (●) X_c, (■) S_{CO} and (▲) S_{CO_2}, the error bars correspond to the uncertainty due to replicate experimental results.
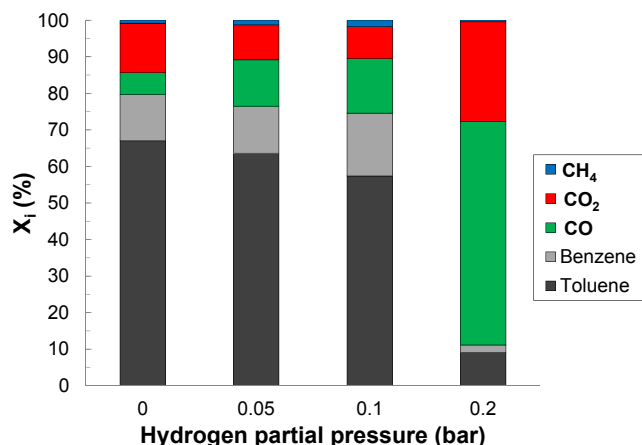
Fig. 7. Effect of hydrogen partial pressure on the normalized distribution of carbon amount during toluene conversion with olivine particles (experiments O_2 with P_{H_2O} = 0.1 bars).

conversion of toluene (experiment O_1). The results show that, in the presence of olivine particles, about 30% of the introduced toluene is converted into carbonaceous compounds such as C_6H_6, CO, CO_2 and CH_4. Besides, it was found that the toluene conversion is independent of the steam partial pressure. The very small amount of CH_4 in the produced gases indicates that benzene is mainly formed according to Reaction (IV). Fig. 6 (B) shows the selectivities of both CO and CO_2 versus steam partial pressure. It was found that the CO selectivity decreases by raising the steam partial pressure while the CO_2 selectivity increases. This evolution is due to the effect of the WGS reaction (Reaction (III)) which is thermodynamically favored when the steam partial pressure increases.

In the second set of experiments, the effect of hydrogen partial pressure on the toluene conversion is examined between 0 and 0.2 bars for a constant steam partial pressure of 0.1 bars. The results are highlighted in Fig. 7. It can be observed that the toluene conversion increases by raising the hydrogen partial pressure. For instance, with 0.2 bars of hydrogen partial pressure and 0.1 bars of steam partial pressure, 91% of toluene is converted essentially into CO and CO_2 while a very small amount of benzene is detected. This indicates that Reactions (IV) and (V) are no longer favored with this operating condition. The produced CO and CO_2 are mainly from the reactions of steam reforming of toluene and the WGS reaction.

From results given in Fig. 7, it seems that both steam and hydrogen partial pressures play a significant role in toluene conversion over olivine. Therefore, experiments O_2 and O_3 were combined in order to emphasize the effect of P_{H_2}/P_{H_2O} on toluene conversion at 850 °C with olivine. The results are given in Fig. 8(A) and (B). Several conclusions can be drawn:

- For $P_{H_2}/P_{H_2O} \leqslant 1$, a constant toluene conversion of about 40% is obtained with the presence of a non-negligible amount of benzene in the output gas. The reactions of hydrodealkylation and steam dealkylation as well as the WGS reaction are favored and lead to the formation of C_6H_6, CO, CO_2 and CH_4.
- For $P_{H_2}/P_{H_2O} = 2$, a toluene conversion of 90% is obtained. A very small amount of benzene and CH_4 is produced which emphasizes that olivine catalyzes the reaction of steam reforming (Reaction (II)).
- Finally, for $P_{H_2}/P_{H_2O} = 4$, less than 1% of toluene is not converted. The carbonaceous products detected are CO and CO_2 and a very small amount of CH_4. Besides, the selectivity of benzene strongly decreases to 0.
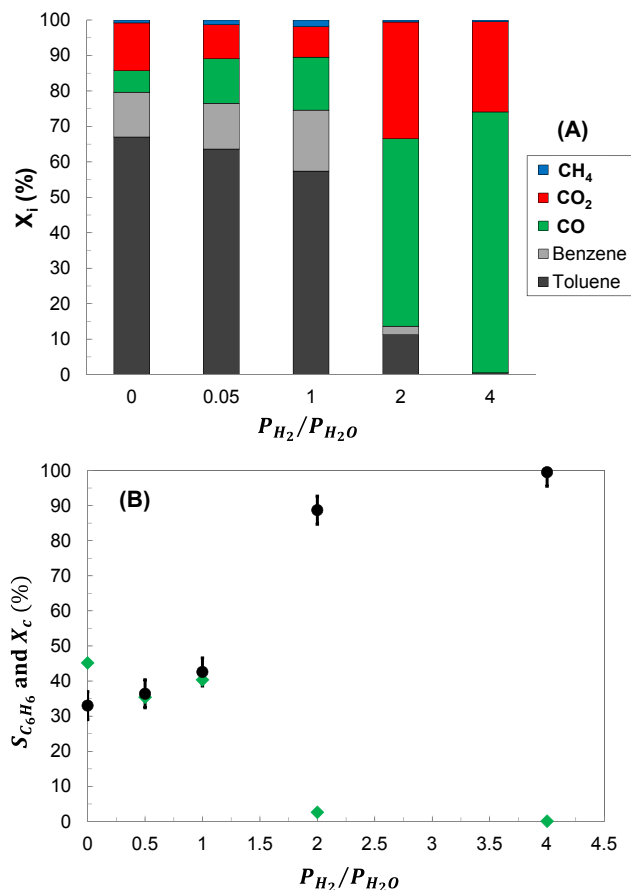

Fig. 8. Effect of P_{H_2}/P_{H_2O} ratio on toluene conversion, (A) Normalized distribution of carbon-containing products, (B) Selectivities of benzene and toluene conversion (●) X_c and (◆) $S_{C_6H_6}$, the error bars correspond to the uncertainty due to replicate experimental results.

3.3. Characterization of olivine particles

In order to highlight the catalytic effect of olivine, characterization of this material after a test with P_{H_2} = 0.2 bars and P_{H_2O} = 0.05 bars (experiment O_3d) was performed using EDX and XRD analyses. In this condition, P_{H_2}/P_{H_2O} is equal to 4. According to Fig. 8, olivine showed a strong catalytic activity towards toluene conversion. In the following, this olivine sample will be referred to "reduced olivine". The results are compared to those obtained with calcined olivine.

3.3.1. EDX analysis

Fig. 9 presents a SEM picture of a calcined olivine particle in which EDX analysis is performed on the surface of a grain. The atomic distribution of iron, oxygen, magnesium and silicon is given along a line and shows a significant variation of each compound. However, oxygen is always present in large excess which suggests that, in the case of calcined olivine, iron is mainly oxidized.

The EDX analysis along a line of the reduced olivine particle is given in Fig. 10. It can be seen that, on the first 10 μm along the line, iron is the only detected element without any oxygen traces. From 10 μm to 25 μm, magnesium, silicon and iron are detected but oxygen is no longer in large excess compared to Fig. 9. Therefore, the reduced olivine sample may contain some traces of native iron (Fe^0) on its surface. This Fe^0 might be formed by iron reduction on olivine surface under reducing atmosphere with $P_{H_2}/P_{H_2O} \geqslant 2$.

3.3.2. XRD analysis

Fig. 11 presents the comparison between the XRD spectra of calcined and reduced olivine in the 2θ = 10–50° range. The data indicate
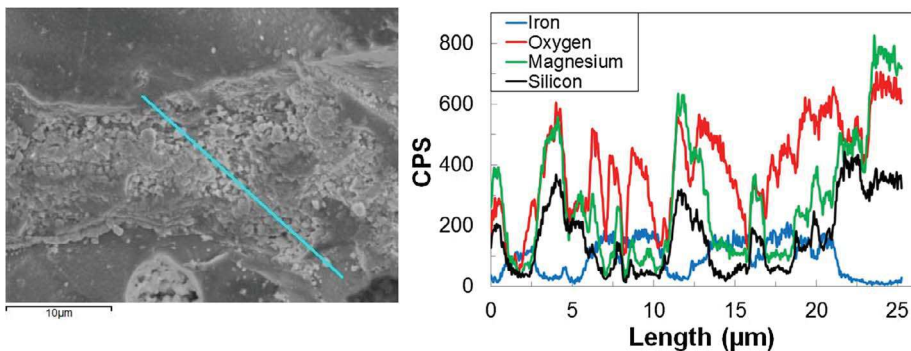
Fig. 9. SEM picture and EDX analysis of an iron-rich zone along a line on the calcined olivine surface.

that the main diffraction peaks of both calcined and reduced olivine are characteristic of the forsterite phase (Mg_2SiO_4). Additional peaks were also observed which correspond to secondary crystalline phases including enstatite ($Mg_2Si_2O_6$) observed at $2\theta = 28.1°$ and $31.1°$ [39] and hematite (Fe_2O_3) at $2\theta = 33.2°$. A moderate peak at $42°$ also appears on both the reduced and the calcined olivine spectra which can be attributed to the presence of FeO [17]. Michel et al. [39] also mentioned that, after olivine calcination, numerous phases of iron oxide are present such as γ-Fe_2O_3, α-Fe_2O_3, Fe_3O_4, or $MgFe_2O_4$ which are difficult to distinguish by X-ray diffraction.

The feature of interest in these spectra is the strong peak at $2\theta = 44.5°$ observed on the reduced olivine sample. This band corresponds to metallic iron ($\alpha-Fe$) [40,41] and is associated with the presence of native iron (Fe^0) on the particle surface.

Therefore, the comparison between XRD spectra of calcined and reduced olivine highlighted the presence of characteristic peaks of olivine structure on both spectra. However, a strong peak corresponding to metallic iron ($\alpha-Fe$) was detected for the reduced olivine which suggests that this sample contains a large amount of native iron Fe^0 on its surface.

3.3.3. Thermodynamic equilibrium of iron

The thermodynamic equilibrium of iron versus P_{H_2}/P_{H_2O} ratio is given in Fig. 12 for a constant temperature of 850 °C. Two zones can be emphasized in the figure. First, for a P_{H_2}/P_{H_2O} ratio up to 1.5, FeO is the main oxidized specie. In this case, olivine showed a low catalytic activity. For P_{H_2}/P_{H_2O} ratios above 1.5, native Fe (Fe^0) becomes the predominant element and olivine has a very significant catalytic effect. These results are in good agreement with experimental data given in Fig. 8 and XRD spectra of Fig. 11 which report that, for a P_{H_2}/P_{H_2O} ratio higher than 2, native iron is present on the olivine surface and catalyzes the steam reforming reaction of toluene.

3.4. Mechanism of toluene decomposition and olivine oxidation/reduction

At 850 °C, olivine showed a strong catalytic activity in steam reforming of toluene for a P_{H_2}/P_{H_2O} ratio higher than 2. Characterization

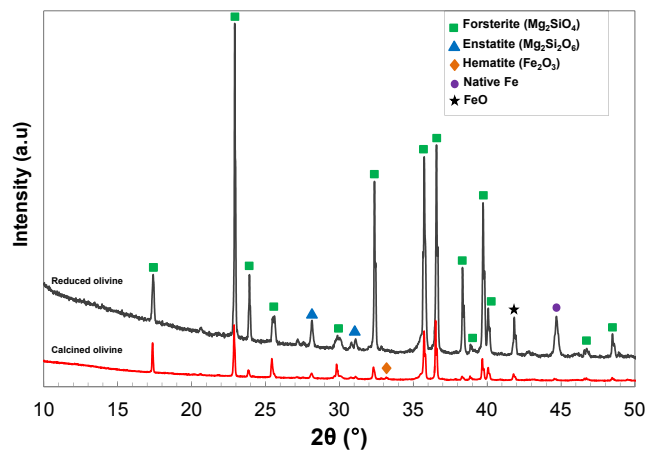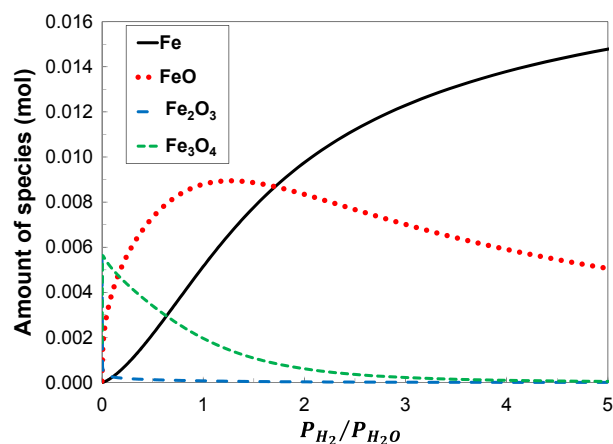Fig. 11. XRD analysis of calcined and reduced olivine.

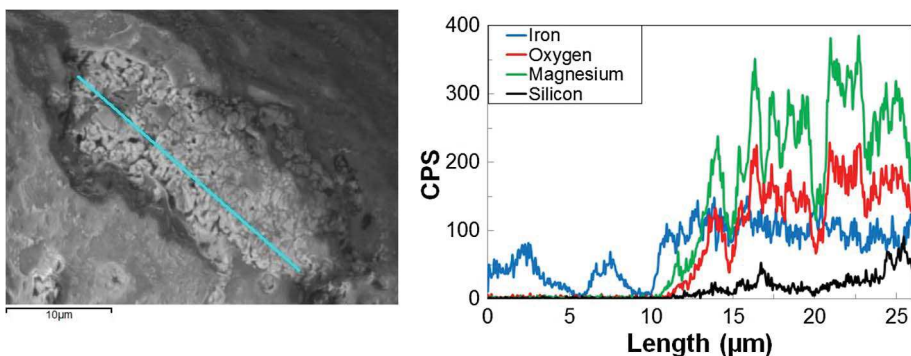Fig. 12. Thermodynamic equilibrium of iron at 850 °C versus P_{H2}/P_{H2O} ratio.

Fig. 10. SEM picture and EDX analysis of an iron-rich zone along a line on the olivine surface particle recovered after experiment O_3d.
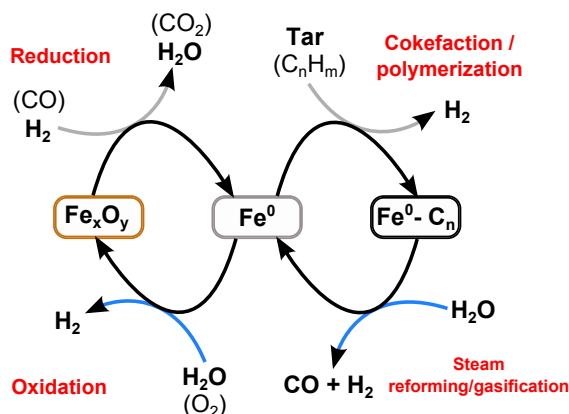
Fig. 13. Schematic diagram of the catalytic mechanism of tars conversion over olivine.

of olivine by EDX and XRD analyses combined to the thermodynamic equilibrium of iron revealed that the presence of native iron Fe^0 is responsible of the catalytic activity of olivine. Besides, several works in the literature [14,29] mentioned that tars conversion over an iron catalyst occurs in two steps: the tars polymerization on the catalyst surface followed by the steam gasification/reforming of the carbonaceous deposit.

Fig. 13 presents a schematic diagram of the catalytic mechanism of tars conversion over olivine. It can be divided into four steps.

(i) Reduction step: for P_{H_2}/P_{H_2O} ratios higher than 1.5, the reactive atmosphere is reducing enough to form native iron on the olivine surface. Fe_xO_y is then reduced to native Fe^0. This reduction step may also take place in the presence of carbon monoxide.

(ii) Polymerization step: the reduced iron active sites at the olivine surface catalyze the reaction of polymerization of toluene which leads to a carbonaceous solid deposition on the catalyst. This step yields to a large formation of hydrogen.

(iii) Steam reforming/gasification step: The produced carbonaceous deposit reacts with steam to produce CO and H_2 by steam reforming or gasification of carbon. The WGS reaction may also occur in the gas phase to produce CO_2.

(iv) Finally, in the presence of oxidizing atmosphere (i.e. large amount of H_2O or oxygen), the native iron is oxidized which gives rise to iron with different oxidation step (Fe(III), Fe(II) and Fe^0).

Consequently, during biomass gasification in FICFB process, it is essential to carefully control the amount of H_2O and H_2 in the gasifier in order for the gas atmosphere to be reducing enough to form native iron on the olivine surface. In this case, tars conversion in the gasifier would be catalyzed by olivine particles and would reduce the amount of tars in the process output. This might be carried out by reinjecting the product syngas in the gasifier which would lead to an increase in the reducing gas atmosphere and a decrease in the steam partial pressure.

4. Conclusion

This paper presented a study of tar conversion over olivine and sand in a fluidized bed reactor using toluene as tar model. The effect of the solid medium (sand or olivine) and of the reactive atmosphere was investigated in order to understand the influence of H_2 and H_2O on the catalytic activity of olivine.

Experiments were performed at 850 °C and atmospheric pressure for steam partial pressures between 0.05 and 0.4 bars and hydrogen partial pressures in the range of 0 to 0.2 bars.

Results showed that, in the presence of sand particles in the reactor, the steam partial pressure has no effect on toluene conversion. The addition of hydrogen in the reactive atmosphere leads to a partial

toluene conversion by hydrodealkylation reaction to produce large amounts of benzene. In the presence of olivine particles in the fluidized bed, the steam partial pressure gave rise to toluene conversion by steam dealkylation reactions.

Besides, it was found that toluene conversion was substantially improved by adding hydrogen in the gas atmosphere. In particular, the catalytic effect of olivine was related to the P_{H_2}/P_{H_2O} ratio in the reactor. When $P_{H_2}/P_{H_2O} > 1.5$, the gas is reducing enough to form reduced iron active sites (Fe^0) on the olivine surface which catalyzes the steam reforming of toluene. For a $P_{H_2}/P_{H_2O} = 4$, 99.5% of the carbon content in the introduced toluene is converted into CO and CO_2.

Finally, on the basis of literature data, a schematic diagram of the catalytic mechanism of tars conversion over olivine was proposed. It indicates that steam reforming of toluene is catalyzed by the presence of native iron and is divided into two steps: the tars polymerization at the olivine surface leading to the formation of a carbonaceous solid followed by the steam reforming or gasification of the solid deposit.

References

[1] Di Blasi C. Modeling chemical and physical processes of wood and biomass pyrolysis. Prog Energy Combust Sci 2008;34:47–90.
[2] Milne TA, Evans RJ. Biomass gasifier "tars": their nature, formation, and conversion. National Renewable Energy Laboratory 1998; 1998.
[3] Bridgwater AV. Renewable fuels and chemicals by thermal processing of biomass. Chem Eng J 2003;91:87–102.
[4] de Sousa L. Gasification of wood, urban wastewood (Altholz) and other wastes in a fluidized bed reactor PhD Thesis 2001; 2001.
[5] Devi L, Ptasinski KJ, Janssen FJJG. A review of the primary measures for tar elimination in biomass gasification processes. Biomass Bioenergy 2003;24:125–40.
[6] Kirnbauer F, Wilk V, Hofbauer H. Performance improvement of dual fluidized bed gasifiers by temperature reduction: the behavior of tar species in the product gas. Fuel 2013;108:534–42.
[7] Sutton D, Kelleher B, Ross JRH. Review of literature on catalysts for biomass gasification. Fuel Process Technol 2001;73:155–73.
[8] Dayton D. A review of the literature on catalytic biomass tar destruction, Milestone Completion Report; 2002.
[9] El-Rub ZA, Bramer EA, Brem G. Review of catalysts for tar elimination in biomass gasification processes. Ind Eng Chem Res 2004;43:6911–9.
[10] Corella J, Toledo JM, Padilla R. Olivine and dolomite as in-bed additive in biomass gasification with air in a fluidized bed reactor: which is better? Energy Fuels 2004;18:713–20.
[11] Simell P, Kurkela E, Ståhlberg P, Hepola J. Catalytic hot gas cleaning of gasification gas. Catal Today 1996;27:55–62.
[12] Rapagnà S, Jand N, Kiennemann A, Foscolo PU. Steam-gasification of biomass in a fluidized-bed of olivine particles. Biomass Bioenergy 2000;19:187–97.
[13] Olivares A, Aznar MP, Caballero MA, Gil J, Francés E, Corella J. Biomass gasification: produced gas upgrading by in-bed use of dolomite. Ind Eng Chem Res 1997;36:5220–6.
[14] Nitsch X, Commandré JM, Clavel P, Martin E, Valette J, Volle G. Conversion of phenol-based tars over olivine and sand in a biomass gasification atmosphere. Energy Fuels 2013;27:5459–65.
[15] Devi L, Craje M, Thüne P, Ptasinski KJ, Janssen FJJG. Olivine as tar removal catalyst for biomass gasifiers: catalyst characterization. Appl Catal A General 2005;294:68–79.
[16] Devi L, Ptasinski KJ, Janssen FJJG, van Paasen SVB, Bergman PCA, Kiel JHA. Catalytic decomposition of biomass tars: use of dolomite and untreated olivine. Renewable Energy 2005;30:565–87.
[17] Kuhn JN, Zhao Z, Felix LG, Slimane RB, Choi CW, Ozkan US. Olivine catalysts for methane- and tar-steam reforming. Appl Catal B 2008;81:14–26.
[18] Miccio F, Piriou B, Ruoppolo G, Chirone R. Biomass gasification in a catalytic fluidized bed reactor with beds of different materials. Chem Eng J 2009;154:369–74.
[19] de Andrés JM, Narros A, Rodríguez ME. Behaviour of dolomite, olivine and alumina as primary catalysts in air-steam gasification of sewage sludge. Fuel 2011;90:521–7.
[20] Koppatz S, Pfeifer C, Hofbauer H. Comparison of the performance behaviour of silica sand and olivine in a dual fluidized bed reactor system for steam gasification of biomass at pilot plant scale. Chem Eng J 2011;175:468–83.
[21] Christodoulou C, Grimekis D, Panopoulos KD, Pachatouridou EP, Iliopoulou EF, Kakaras E. Comparing calcined and un-treated olivine as bed materials for tar reduction in fluidized bed gasification. Fuel Process Technol 2014;124:275–85.
[22] Göransson K, Söderlind U, Engstrand P, Zhang W. An experimental study on catalytic bed materials in a biomass dual fluidized bed gasifier. Renewable Energy

2015;81:251–61.

[23] Erkiaga A, Lopez G, Amutio M, Bilbao J, Olazar M. Steam gasification of biomass in a conical spouted bed reactor with olivine and γ-alumina as primary catalysts. Fuel Process Technol 2013;116:292–9.

[24] Świerczyński D, Courson C, Bedel L, Kiennemann A, Vilminot S. Oxidation reduction behavior of iron-bearing olivines (FexMg1-x)2SiO4 used as catalysts for biomass gasification. Chem Mater 2006;18:897–905.

[25] Virginie M, Courson C, Niznansky D, Chaoui N, Kiennemann A. Characterization and reactivity in toluene reforming of a Fe/olivine catalyst designed for gas cleanup in biomass gasification. Appl Catal B 2010;101:90–100.

[26] Virginie M, Libs S, Courson C, Kiennemann A. Iron/olivine catalysts for tar reforming: comparison with nickel/olivine. In: Zakopane 2008: Catalysis for environment: depollution, renewable energy and clean fuel; 2008.

[27] Polychronopoulou K, Bakandritsos A, Tzitzios V, Fierro JLG, Efstathiou AM. Absorption-enhanced reforming of phenol by steam over supported Fe catalysts. J Catal 2006;241:132–48.

[28] Nordgreen T, Liliedahl T, Sjöström K. Metallic iron as tar breakdown catalyst related to atmospheric, fluidized bed gasification of biomass. Fuel 2006;85:689–94.

[29] Uddin MdA, Tsuda H, Wu S, Sasaoka E. Catalytic decomposition of biomass tars with iron oxide catalysts. Fuel 2008;87:451–9.

[30] Świerczyński D, Libs S, Courson C, Kiennemann A. Steam reforming of tar from a biomass gasification process over Ni/olivine catalyst using toluene as a model compound. Appl Catal B 2007;74:211–22.

[31] Yung MM, Magrini-Bair KA, Parent YO, Carpentier DL, Feik CJ, Gaston KR, et al. Demonstration and characterization of Ni/Mg/K/AD90 used for pilot-scale conditioning of biomass-derived syngas. Catal Lett 2010;134:242–9.

[32] Caballero MA, Aznar MP, Gil J, Martin JA, Francés E, Corella J. Commercial steam reforming catalysts to improve biomass gasification with steam-oxygen mixtures. 1. Hot gas upgrading by the catalytic reactor. Ind Eng Chem Res 1997;36:5227–39.

[33] Taralas G, Kontominas MG. Kinetic modelling of VOC catalytic steam pyrolysis for tar abatement phenomena in gasification/pyrolysis technologies. Fuel 2004;83:1235–45.

[34] Taralas G, Kontominas MG. Numerical modeling of tar species/VOC dissociation for clean and intelligent energy production. Energy Fuels 2005;19:87–93.

[35] Taralas G, Kontominas MG, Kakatsios X. Modeling the thermal destruction of toluene (C_7H_8) as tar-related species for fuel gas cleanup. Energy Fuels 2003;17:329–37.

[36] Hasler P, Nussbaumer Th. Gas cleaning for IC engine applications from fixed bed biomass gasification. Biomass Bioenergy 1999;16:385–95.

[37] Mozaffarian M, Zwart R, Boerrigter H, Deurwaarder E, Kersten S. Green gas as sng (synthetic natural gas) a renewable fuel with conventional quality, ECN-RX-04-085; 2004.

[38] Graham RG, Bain R. Biomass gasification: hot-gas clean-up, International Energy Agency. In: Biomass Gasification Working Group. p. 44.

[39] Michel R, Ramzi Ammar M, Poirier J, Simon P. Phase transformation characterization of olivine subjected to high temperature in air. Ceram Int 2013;39:5287–94.

[40] Fredriksson HOA, Lancee RJ, Thüne PC, Veringa HJ, Niemantsverdriet JW. Olivine as tar removal catalyst in biomass gasification: catalyst dynamic under model conditions. Appl Catal B 2013;130–130:168–77.

[41] Nordgreen T, Nemanova V, Engvall K, Sjöström K. Iron-based materials as tar depletion catalysts in biomass gasification: dependency of oxygen potential. Fuel 2012;95:71–8.